

**METAL IN UREILITES: PETROLOGIC CHARACTERIZATION.** <sup>1</sup>C.A. Goodrich, <sup>2</sup>J.A. Van Orman, <sup>3</sup>K. Domanik and <sup>4</sup>J.L. Berkley. <sup>1</sup>Dept. of Physical Sciences, Kingsborough Community College, Brooklyn, NY 11235 USA; cgoodrich@kingsborough.edu. <sup>2</sup>Dept. of Geological Sciences, Case Western Reserve University, Cleveland, OH 44120 USA. <sup>3</sup>Lunar and Planetary Laboratory, University of Arizona, Tucson AZ 85721 USA. <sup>4</sup>Dept. of Geosciences, State University of New York, Fredonia NY 14063 USA.

**Introduction:** Many of the petrologic characteristics of ureilites that are difficult to reconcile with normal igneous processes [1] can be explained by a smelting model, in which silicate *mg* (molar Mg/[Mg+Fe]) are controlled by carbon redox reactions [2-4]. However, their metal and siderophile element abundances appear to be inconsistent with such a model [5-7]. The smelting reaction ( $\text{FeO} + \text{C} \rightarrow \text{Fe} + \text{CO}$ ) predicts a correlation of *mg* with metal content, or (if the metal is removed) depletion of siderophile elements. In contrast, ureilites have uniformly low (a few %) metal contents, and relatively high ( $\sim 0.01$ - $1 \times \text{CI}$ ) siderophile element abundances uncorrelated with *mg*. We are addressing this apparent contradiction through petrographic and trace element [8] characterization of metal in ureilites, and petrologic modelling [9].

**Samples and Analytical:** The initial samples studied were olivine + low-Ca pyroxene (lpx) ureilites Kenna (Fo 79), PCA 82506 (Fo 78), ALHA77257 (Fo 85), EET 96328 (Fo 86) and EET 90019 (Fo 89), as well as augite-bearing ureilites META78008 (Fo 76), Hughes 009 (Fo 87) and ALH 82130 (Fo 95). Sections were characterized by SEM at KCC; metal, sulfides and oxidized metal were analyzed by EMPA at LPL.

**Types of Metal:** Based on textures we distinguish 5 types of metal: 1) Metal lining grain boundaries (Fig. 1). In most ureilites this has been partially or completely oxidized, presumably terrestrially; 2) Reduction metal, which occurs in dense patches of sub-micron (occasionally up to 10  $\mu\text{m}$ ) grains in rims and veins in reduced olivine (Fig. 1); 3) Metal enclosed in graphite, either on grain boundaries or within silicates; 4) Sparsely distributed trails of sub-micron grains that occur in both lpx and olivine and are not associated with reduced silicates (Fig. 1); 5)  $\sim 5$ - $150 \mu\text{m}$ -sized carbide-metal-phosphide-sulfide spherules [10], which occur predominantly as inclusions in lpx (rarely olivine). Sulfides show rounded boundaries with the carbide-metal-phosphide assemblages (Fig. 2). The latter consist of cohenite ( $\text{Fe}_3\text{C}$ ) intergrown with metal in a range of grain sizes, with phosphide as rims or dispersed grains (Fig. 2).

Other than in the type 5 spherules, sulfides are very rare. In all samples, grain boundary metal (or oxide) is the most abundant type. We observed  $>50$  spherules in ALHA77257,104 and  $>50$  in one pigeonite grain alone in PCA 82506,24, but none in Kenna or EET90019 and only 1-2 in each of the other samples. A few grains of metal could not be classified.

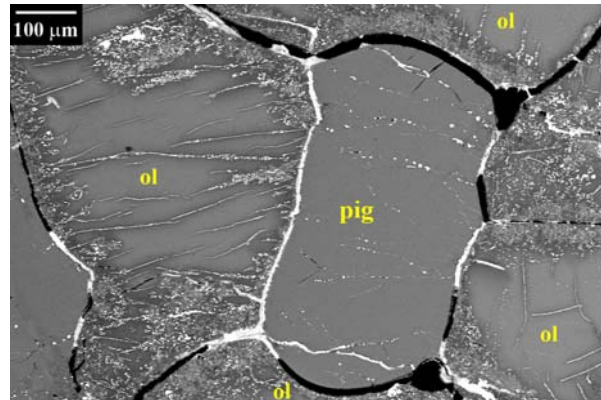


**Fig. 1.** BEI of PCA 82506,24 showing types 1, 2 and 4 metal (white). ol = olivine; pig = pigeonite.

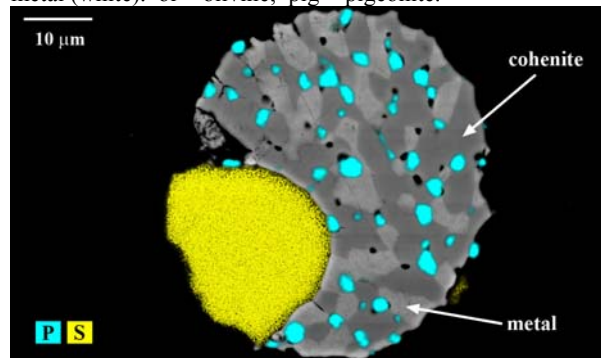


**Fig. 2.** Cohenite-metal-phosphide-sulfide spherule in pigeonite in ALHA77257,104 (aka ,15a). BEI combined with P (cyan) and S (yellow) x-ray maps.

**Compositions:** We obtained data from grain boundary metal in ALHA77257, META78008, ALH 82130 and Hughes 009. Grain boundary metal in our sections of Kenna, EET 96328 and EET 90019 was entirely oxidized. We also obtained data from a few of the larger blebs of type 2 metal, metal in graphite in several samples, and all spherules observed.

**Non-Spherule Metal:** All non-spherule metals analyzed have low abundances of C ( $<0.7\%$ ), P ( $<0.6\%$ ) and S ( $<0.01\%$ ). With the possible exception of grain boundary metal in Hughes 009, they show a positive correlation between Ni ( $\sim 0.5$ - $5.5\%$ ) and Co ( $\sim 0.05$ - $0.5\%$ ), with metal in graphite having the highest values (Fig. 3). Cr shows an increase followed by a decrease with increasing Ni within META78008 and among samples (META78008  $\rightarrow$  ALHA77257  $\rightarrow$  ALH 82130). Si ( $<0.4\%$ ) also increases with increasing Ni within META78008. Si contents of all metal in ALH 82130 are  $\sim 1\%$  (Fig. 3). Grain boundary metal in Hughes 009 is unusual; it consists of a eutectic-like

intergrowth of schreibersite and metal, with a bulk composition (from point counting) of ~9% P (Fig. 3). Of the few blebs of type 2 metal only one is distinct (~0.6% Ni) from grain boundary metal. No unclassified metal is distinct.

**Spherule Metal:** Cohenite contains 1.2-3.7% Ni, 0.2-0.4% Co and 0.06-0.4% Cr. Metal intergrown with coarse cohenite is low-C (<0.7%), with ~5-10% Ni, 0.35-0.65% Co and <0.1% Cr. Some "metal" shows 2-3% C and is likely a fine-grained intergrowth of cohenite and metal [10]. Phosphides appear to be schreibersite, although only a few "clean" analyses were obtained. Sulfides have high Cr (up to ~2.6%). Bulk compositions (excluding sulfide) of 5 spherules in pigeonite were determined by point counting and modal recombination. Results (Fig. 3) are similar to those of [10] but with higher P (phosphides were not visible in 1986 BEI). Compared to grain boundary metal they have high C (~3.6-4%) and P (~1-2%), low-Cr (<0.2%) and similar Co contents (Fig. 3). Broad-beam analyses of fine-grained spherules give similar results but have low totals. Spherules in olivine may have lower Co than those in lpyx.

**Oxidized Metal:** Oxidized metal areas are highly variable mixtures of several Fe-oxides (bulk O = 25-40%), with low Si, Mg, S, P, Ca, Ni and Cl.

**Interpretations:** Only the grain boundary and spherule metal are likely to be primary. Type 2 metal has long been recognized as a product of secondary reduction of olivine, with low Ni [11] supporting this. Our few analyses of some of the larger blebs of metal in reduced olivine suggest that they are not pure reduction metal. Type 4 metal was interpreted as shock-mobilized [12] and we agree with this.

The compositional trends observed for grain boundary metal and metal in graphite (Fig. 3) suggest that secondary reduction may also have altered primary metal compositions by increasing Ni, Co, Si and Cr. The high Si of metal in ALH 82130, which shows one of the highest degrees of secondary reduction [13,14], strongly supports this. The overturn in the Ni-Cr trend may be due to formation of Cr-sulfides or Cr-carbides. This interpretation would imply that only the lowest-Ni compositions are primary.

Spherule metal is texturally and compositionally distinct from grain boundary metal. We interpret it to represent droplets of Fe-S-C-P liquid (subsequently separated into immiscible Fe-S and Fe-Ni-C-P liquids) that were immiscible in silicate melt. Trapping of these spherules predominantly in lpyx supports the smelting model, since in this model only lpyx crystallizes from a melt [2,3]. S, P and C (high in spherules, low in grain boundary metal) and Co (similar in the two

types) contents suggest that grain boundary and spherule metal are solid metal-liquid metal complements. This hypothesis is tested with trace elements [8].

The P-rich grain boundary metal in Hughes 009 appears to be an Fe-P eutectic melt, but is not apparently associated with C- or S-rich melts. It may be shock-remobilized [15].

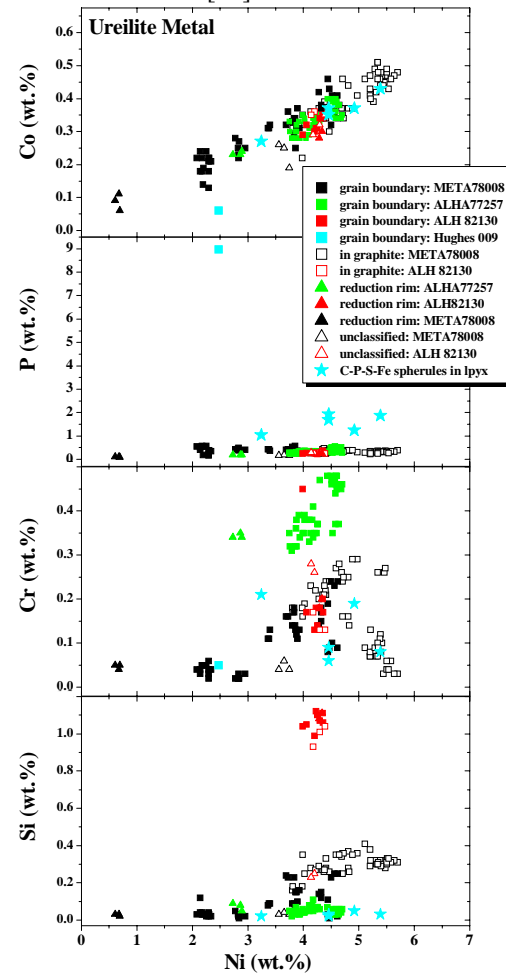


Fig. 3. Compositions of metal in ureilites.

**References:** [1] Mittlefehldt D.W. et al. (1998) In *Planetary Materials, Rev. Mineral.* **36**. [2] Goodrich C.A. et al. (2007) *GCA* **71**, 2876. [3] Singletary S.J. and Grove T.L. (2003) *MAPS* **38**, 95. [4] Walker D. and Grove T.L. (1998) *MAPS* **28**, 629. [5] Mittlefehldt D.W. et al. (2005) *LPS* **36**, #1140. [6] Warren P.H. and Huber H. (2006) *MAPS* **41**, 835. [7] Warren P.H. et al. (2006) *GCA* **70**, 2104. [8] Ash R. et al. (2009) this volume. [9] Van Orman J.A. et al. (2009) this volume. [10] Goodrich C.A. and Berkley J.L. (1986) *GCA* **51**, 2255. [11] Berkley J.L. et al. (1980) *GCA* **44**, 1579. [12] Rubin A.E. (2006) *MAPS* **41**, 125. [13] Berkley J.L. et al. (1985) *Meteorit.* **20**, 607. [14] Takeda H. et al. (1989) *Meteorit.* **24**, 73. [15] Goodrich C.A. et al. (2001) *GCA* **65**, 621.